JOURNAL OF APPLIED PHYSICS VOLUME 95, NUMBER 11 1 JUNE 2004

Peak magnetocaloric effects in Al-Gd-Fe alloys

V. Provenzano, A. J. Shapiro, and R. D. Shull
Magnetic Materials Group, National Institute of Standards and Technology, 100 Bureau Drive, MS-8552, Gaithersburg, Maryland 20899

T. King, E. Canavan, P. Shirron, and M. DiPirro
NASA Goddard Space Flight Center, Code 552, Greenbelt, Maryland 20771

(Presented on 7 January 2004)

The magnetocaloric properties of several $Al_xGd_yFe_z$ (with $x+y+z=100$) ternary alloys have been determined between 2 and 300 K. Three distinct peaks in the magnetic entropy change ΔS_m versus T were found: a low-temperature peak (near 10 K), an intermediate temperature peak (80–160 K), and a higher temperature peak (210 to 280 K). The low-temperature peak coincides with a field-induced antiferromagnetic-to-ferromagnetic transition; the intermediate and high temperature peaks are associated with other magnetic transitions. Above 60 K, these alloys exhibited superparamagnetic behavior and possessed enhanced ΔS_m values, as predicted earlier for magnetic nanocomposites. © *2004 American Institute of Physics.* [DOI: 10.1063/1.1667832]

Magnetic refrigeration, based on the magnetocaloric effect, has created the opportunity for developing an efficient and environmentally friendly cooling technology. In fact, compared to conventional vapor compression refrigeration, magnetic refrigeration can in principle be much more efficient than conventional processes (because of its reversible nature) and it does not rely on ozone-depleting chlorofluorocarbon refrigerants.[1] The magnetocaloric effect is the thermal response of a magnetic material under the application of an external magnetic field. The magnitude of this effect is given by the field-induced entropy change ΔS_m. When a magnetic field is applied to the material there is a decrease in its magnetic entropy due to the alignment of the spins with the field. The reverse takes place upon the removal of the applied field. A change in temperature ΔT follows, and is the basis for magnetic cooling.

In recent years, research and development efforts in the area of magnetic refrigeration have focused on finding materials with improved magnetocaloric effects. These include materials capable of operating at different temperature ranges, depending on the intended application. For example, the work of Gschneidner and Pecharsky and their co-workers at Ames Laboratory has shown that a large magnetocaloric effect (dubbed as the ''giant'' magnetocaloric effect) can be obtained in some gadolinium-silicon-germanium (GdSiGe) alloys.[2] These authors have adjusted the composition of these alloys in order to shift the ferromagnetic (FM) transition temperature (e.g., the temperature of peak ΔS_m) from 30 K to room temperature. A complementary approach has been employed by Shull and his group at NIST to both ''tune'' and enhance the magnetocaloric effect for magnetic refrigeration applications at different temperature ranges by focusing on the development of magnetic nanocomposites.[3,4] These nanocomposites were initially based on gadolinium-gallium garnets with additions of FM transition-metal elements, such as iron.

Low-temperature, as well as high-temperature, applications are envisioned. For near to mid-term astronomical and exploratory missions, NASA in particular needs more efficient low-temperature space-based cooling systems in order to meet more stringent sensitivity and heat transfer requirements in its satellite detector systems. With smaller devices more devices are packed into the same volume and greater cooling is required. NASA also wants to replace its detector array mechanical cryocoolers because they (1) are inefficient below 20 K (only a few percent Carnot efficiency) and (2) are often the source of unwanted vibrations that reduce the detector sensitivities.

The GdFeAl system was selected for the present study because of the ''mictomagnetic'' state previously discovered in Fe-Al alloys.[5] Such a system is comprised of FM clusters and possesses superparamagnetic character in certain temperature ranges. In addition, recent work on FeAl alloys has also shown these materials to possess spin density waves[6] which, it was felt, should also contribute to the magnetothermal effects in the system. The addition of Gd was expected to form magnetic clusters with much larger magnetic moments because of the larger moment of the Gd atom, thereby contributing to much enhanced magnetocaloric effects as predicted for magnetic nanocomposites.[3]

Various Al-Gd-Fe alloy samples were prepared in this study by arc melting, using a water-cooled copper hearth in an argon atmosphere under ambient pressure, starting with the appropriate amounts of the component elements. The purity of the starting constituents was a mass fraction of 99.9% or better. Magnetic measurements were conducted on alloy

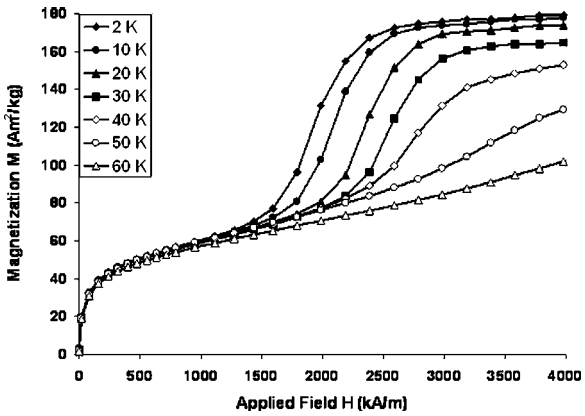

FIG. 1. Magnetization vs field curves (2–60 K) of the $Al_{28}Gd_{60}Fe_{12}$ alloy, in the as-cast condition. The curves show a rapid rise in the magnetization for field values above 1.59 MA/m (2 T), indicative of a field-induced first order magnetic phase transition.

samples in the as-cast condition. The microstructure of the samples was characterized by SEM.

The magnetocaloric responses of the alloy samples were determined by measuring their magnetization M as a function of temperature and applied magnetic field using a super conducting quantum interference device (SQUID) magnetometer. The magnetization M was measured at discrete temperature intervals from 2 to 360 K and at discrete magnetic field intervals ranging from 0 to 3.98 MA/m (5 T). M was normalized to the sample mass, and the magnetic entropy change (ΔS_m) was calculated from the integrated Maxwell relation and the magnetization data. That is,

$$\left(\frac{\partial S}{\partial H}\right)_T = \left(\frac{\partial M}{\partial T}\right)_H. \tag{1}$$

Integration of this expression leads to

$$\Delta S_m(T,\Delta S) = \int_0^{H'} \left(\frac{\partial M}{\partial T}\right)_H dH. \tag{2}$$

In Eqs. (1) and (2), M represents the magnetization, T the temperature, and H the applied magnetic field. For magnetization measurements made at constant temperature at discrete magnetic field intervals, this Maxwell expression can be approximated by the following expression:

$$\Delta S_m \approx \frac{1}{\Delta T}\left[\int_0^{H'} M(T+\Delta T,H)dH - \int_0^{H'} M(T,H)dH\right]. \tag{3}$$

Therefore, using the approximation given by Eq. (3), ΔS_m as a function of temperature for each sample was computed numerically by first differentiating the magnetization data M with respect to temperature and then integrating the resulting derivatives from zero field to some value H up to 3.98 MA/m (5 T). The experimental uncertainty of magnetization measurements as well as that the magnetic entropy change (ΔS_m) values calculated from the magnetization data are roughly equal to the symbol sizes in their respective plots.

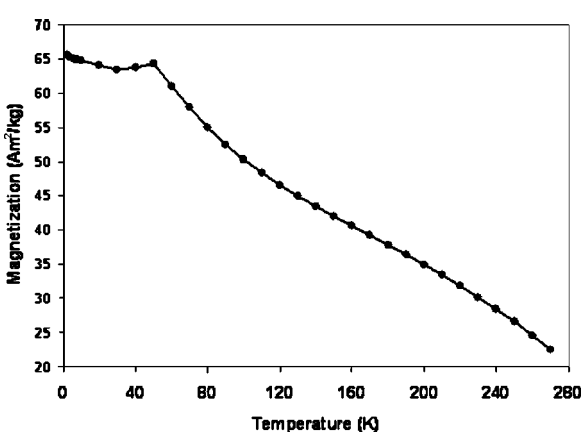

FIG. 2. Magnetization vs temperature curve at a fixed field value of 1.27 MA/m (1.6 T) of the $Al_{28}Gd_{60}Fe_{12}$ alloy, in the as-cast condition, showing the presence of a small peak near 50 K, indicative of two different magnetic phases.

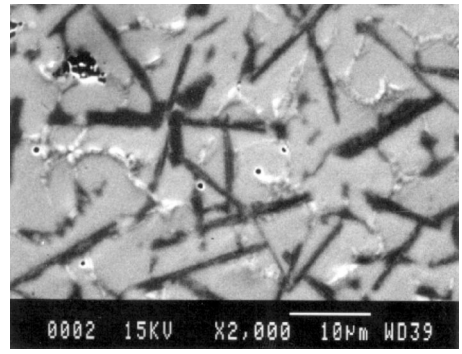

FIG. 3. Backscattered SEM micrograph showing the typical microstructure of the $Al_{28}Gd_{60}Fe_{12}$ alloy, in the as-cast condition. The microstructure indicates the presence of three distinct phases.

The magnetization versus field curves for $Al_{28}Gd_{60}Fe_{12}$ at various temperatures (2–60 K) are presented in Fig. 1. These curves were generated from magnetic data taken with increasing applied field. Although not shown, the companion curves taken with decreasing field are very similar as there was not much hysteresis in the data. Within this temperature range, the magnetization versus field curves show that this alloy exhibits different magnetic behavior below and above $\mu_o H = 1.59$ MA/m (2 T) (μ_o = the magnetic permeability of free space). In fact, below 2 T, the magnetization exhibits FM behavior, whereas above 1.59 MA/m (2 T), the magnetization increases rapidly followed by an approach to saturation at $\mu_o H = 3.18$ MA/m (4 T). The rapid rise in magnetization at $\mu_o H = 1.59$ MA/m (2 T) is likely the result of a field-induced first-order magnetic phase transition. Figure 1 indicates that this first-order transition occurs at higher field values with increasing temperature. The overall magnetization behavior of this alloy is similar to that observed by Li[7] on the Gd_2Al alloy and is consistent with the initial presence of two distinct magnetic phases: a FM phase and an antiferromagnetic (AF) second phase. Upon field application, the antiferromagnet transforms into a ferromagnet at temperatures between 2 and 60 K (for $\mu_o H < 5$ T). Above this temperature range, the alloy exhibits superparamagnetic behavior, indicative of small isolated FM clusters, up to about 200 K, above which it becomes paramagnetic. The M versus T data [at a constant field of $\mu_o H = 1.27$ MA/m (1.6 T)] in Fig. 2 also shows the presence of a small peak near 50 K, indicative of the presence of an AF transition. Furthermore, exami-

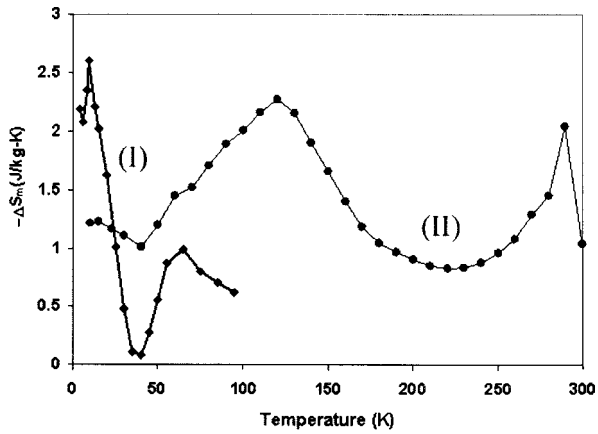

FIG. 4. Computed ΔS_m, normalized with respect to sample mass and integrated over an applied field, $\Delta H = 2.39$ MA/m (3 T), of the (I) $Al_{28}Gd_{60}Fe_{12}$ and (II) $Al_{33}Gd_{45}Fe_{22}$ alloys in the as-cast condition, plotted as a function of temperature.

nation of the alloy microstructure by high-resolution SEM, showed the presence of three chemically distinct phases (Fig. 3): a dominant matrix gray phase whose average composition is $Al_{26}Gd_{71}Fe_3$; a dark minor phase with an average composition of $Al_{32}Gd_{39}Fe_{30}$, and a light-colored phase that was composed mostly of gadolinium with some aluminum, but no iron. It is believed that the $Al_{26}Gd_{71}Fe_3$ is the phase that undergoes the AF/FM first-order phase transition above 2 T.

The ΔS_m values plotted as function of temperature for the $Al_{28}Gd_{60}Fe_{12}$ alloy are presented in Fig. 4. Using both Eqs. (2) and (3), the values of ΔS_m were calculated by numerical differentiation and integration of the corresponding magnetization data. The ΔS_m versus temperature curve shows the presence of two peaks: one larger peak centered at about 10 K and a smaller peak centered around 65 K. Although not shown for the sake of brevity, $Al_{33}Gd_{55}Fe_{12}$ and $Al_{30}Gd_{67}Fe_3$ alloys exhibited a magnetic behavior similar to that of $Al_{28}Gd_{60}Fe_{12}$ alloy. That is, in the 2–60 K temperature range, both alloys showed the presence of a first-order field-induced phase transition above 2 T. In addition as observed in the $Al_{28}Gd_{60}Fe_{12}$ alloy, the transition occurs at higher field values with increasing temperature. The corresponding ΔS_m versus temperature curves showed the presence of two peaks: a low-temperature peak (respectively centered at 5 K for the $Al_{33}Gd_{55}Fe_{12}$ alloy and at 10 K for $Al_{28}Gd_{67}Fe_3$) and an intermediate-temperature peak centered at about 50 K for both alloys. For the three alloy samples and for $\Delta \mu_o H = 1.59$ MA/m (2 T), the maximum ΔS_m value for the lower-temperature peak was 2.5–2.8 J/Kg K, whereas for the higher temperature peak, the maximum value was 0.6–1.2 J/Kg K. The magnitudes and locations of ΔS_m peaks calculated using the Maxwell relations, as done here, may not be exact for systems exhibiting first-order transitions (e.g., in an AF/FM transition), but the temperature variation of ΔS_m would still show the same trends.[8] Consequently, magnetic data is used here as a screening tool in these systems, to be followed up by more definitive calorimetric measurements at some later time.

Similar to that observed in the three alloys just discussed, the magnetization versus field curves up to 60 K for an alloy sample of composition of $Al_{33}Gd_{45}Fe_{22}$ also indicated the presence of a field-induced AF/FM transition above $\mu_o H = 1.59$ MA/m (2 T). However, the strength of this transition was smaller than in the three previously described alloys. The corresponding ΔS_m versus T curve, for $\Delta \mu_o H = 2.39$ MA/m (3 T), showed, in addition to the lower- and the intermediate-temperature peaks previously observed, the presence of a third peak centered near the much higher temperature of 210 K. However, for $Al_{33}Gd_{45}Fe_{22}$ the two low-temperature peaks had shifted up in temperature to 20 and 60 K, respectively. When the alloy composition was changed to $Al_{45}Gd_{45}Fe_{10}$, the corresponding magnetic data showed a much weaker field-induced magnetic transition in the 2 to 40 K temperature range [$\mu_o H = 1.59$ MA/m (2 T)]. In addition, the corresponding ΔS_m versus temperature curve for $\Delta \mu_o H = 3.98$ MA/m (5 T) (Fig. 4) showed the high-temperature peak, first observed for the $Al_{33}Gd_{45}Fe_{22}$ alloy, had shifted from 210 K to between 280 and 290 K. In addition, the intermediate-temperature peak had shifted to a slightly higher temperature.

The field-induced first-order magnetic phase transition was not observed for the following alloy compositions: Al_2Gd, $Al_{50}Gd_{40}Fe_{10}$, and $Al_{50}Gd_{33}Fe_{17}$. Although not shown, the ΔS_m versus T curve [$\Delta \mu_o H = 2.39$ MA/m (3 T)] for these three alloy samples showed only the presence of a single intermediate-temperature peak centered at 100, 120, and 160 K for Al_2Gd, $Al_{50}Gd_{40}Fe_{10}$, and $Al_{50}Gd_{33}Fe_{17}$ respectively. In these three alloys, the peak value of ΔS_m varied between 3.5 and 4.5 J/Kg K for $\Delta \mu_o H = 2.39$ MA/m (3 T).

Superparamagnetism was found in several alloys around the $Al_{28}Gd_{60}Fe_{12}$ composition between 40 and 200 K. As a consequence, peaks in the magnetocaloric effect were also found in that temperature range, consistent with such enhancements found in other magnetic nanocomposites. In addition, a much larger ΔS_m peak was found at temperatures near 10 K, due to the presence of a field-induced AF/FM phase transformation on one of the crystallographic phases making up this composition. This latter peak is particularly attractive for low-temperature magnetic cooling. Alloys with less Gd and more Al (e.g., $Al_{45}Gd_{45}Fe_{10}$) resulted in the development of a near-room-temperature ΔS_m peak.

This work was partially supported by NASA-Goddard Space Flight Center DDF Grant No. S15695Y. The authors are very grateful to Rosetta Drew for her assistance in performing the magnetic measurements.

[1] O. Tegus *et al.*, Nature (London) **415**, 150 (2002).
[2] V. K. Pecharsky and K. A. Gschneidner, Jr., Appl. Phys. Lett. **70**, 3299 (1997); V. K. Pecharsky and K. A. Gschneidner, Jr., *Advances in Cryogenic Engineering*, edited by P. Kittel (Plenum, New York, 1998), Vol. 43.
[3] R. D. Shull. L. J. Swartzendruber, and L. H. Bennett, *Proceedings of The Sixth International Cryocoolers Conference*, edited by G. Green and M. Knox (David Taylor, Annapolis, MD, 1991), p. 231.
[4] R. D. Shull, AIP Conf. Proc. **273**, 628 (1993); R. D. McMichael, J. J. Ritter, and R. D. Shull, J. Appl. Phys. **73**, 6946 (1993); R. D. McMichael *et al.*, J. Magn. Magn. Mater. **111**, 29 (1992).
[5] R. D. Shull *et al.*, Solid State Commun. **20**, 863 (1976).
[6] D. R. Noakes, A. S. Arrott, M. G. Belk, S. C. Deevi, J. W. Lynn, R. D. Shull, and D. Wu, Phys. Rev. Lett. **91**, 217201 (2003).
[7] X. Li, J. Alloys Compd. **288**, 76 (1999).
[8] A. Giguere *et al.*, J. Phys.: Condens. Matter **11**, 6969 (1999).